Published in final edited form as:
Glia. 2014 July ; 62(7): 1162–1175. doi:10.1002/glia.22671.

Voltage-gated sodium channel $Na_v1.5$ contributes to astrogliosis in an *in vitro* model of glial injury via reverse Na^+/Ca^{2+} exchange

Laura W. Pappalardo[1,2,3], **Omar A. Samad**[1,2,3], **Joel A. Black**[1,2], and **Stephen G. Waxman**[1,2]

[1]Department of Neurology and Center for Neuroscience and Regeneration Research, Yale University School of Medicine, New Haven, CT 06510, USA

[2]Rehabilitation Research Center, VA Connecticut Healthcare System, West Haven, CT, 06516, USA

Abstract

Astrogliosis is a prominent feature of many, if not all, pathologies of the brain and spinal cord, yet a detailed understanding of the underlying molecular pathways involved in the transformation from quiescent to reactive astrocyte remains elusive. We investigated the contribution of voltage-gated sodium channels to astrogliosis in an *in vitro* model of mechanical injury to astrocytes. Previous studies have shown that a scratch injury to astrocytes invokes dual mechanisms of migration and proliferation in these cells. Our results demonstrate that wound closure after mechanical injury, involving both migration and proliferation, is attenuated by pharmacological treatment with tetrodotoxin (TTX) and KB-R7943, at a dose that blocks reverse mode of the Na^+/Ca^{2+} exchanger (NCX), and by knockdown of $Na_v1.5$ mRNA. We also show that astrocytes display a robust $[Ca^{2+}]_i$ transient after mechanical injury and demonstrate that this $[Ca^{2+}]_i$ response is also attenuated by TTX, KB-R7943, and $Na_v1.5$ mRNA knockdown. Our results suggest that $Na_v1.5$ and NCX are potential targets for modulation of astrogliosis after injury via their effect on $[Ca^{2+}]_i$.

Keywords

glial scar; sodium channels; sodium-calcium exchanger; migration; proliferation

Introduction

Astrocytes outnumber neurons in the brain and spinal cord and respond to insult in the CNS through the incompletely understood process of reactive astrogliosis, which is a hallmark of the response to injury in many CNS pathologies. While the functional ramifications of astrogliosis are controversial, recent studies suggest that astrocytes can exert both beneficial and detrimental effects, the outcome of which is determined by specific signaling cascades

Address for Correspondence: Stephen G. Waxman, M.D., Ph.D., Neuroscience and Regeneration Research Center VA Connecticut Healthcare System, 950 Campbell Avenue, Bldg. 34 West Haven, CT 06516, Tel: (203) 937-3802, Fax: (203) 937-3801, stephen.waxman@yale.edu.

[3]Authors contributed equally to this work.

The authors declare no competing financial interests.

involved (Sofroniew, 2009), temporal sequence (Rolls et al., 2009), and extent and type of injury, which determine reactive astrocyte phenotype (Zamanian et al., 2012). Astrogliosis can be regarded as a continuum; however, once the process approaches the severe end of the spectrum, the formation of a scar is long-lasting and can inhibit the regeneration of injured neurons (Silver and Miller, 2004; Sofroniew, 2009).

Along with increasing recognition of the importance of astrocytes in CNS pathology, the past 20 years have seen a paradigm shift from the view of astrocytes as traditionally non-excitable cells to the recognition that astrocytes exhibit excitability by way of ionic fluxes, and particularly in the form of $[Ca^{2+}]_i$ oscillations. Astroglial $[Ca^{2+}]_i$ fluxes lead to activation of secretory machinery and exocytosis of neurotransmitters, which can modulate neuronal synapses, a phenomenon that has been termed “gliotransmission” (Agulhon et al., 2008). Aside from modulation of synaptic transmission, levels of intracellular Ca^{2+} are critical for numerous homeostatic cellular functions in astrocytes, including migration and proliferation (Stanimirovic et al., 1995; Wang et al., 2010; Parnis et al., 2013). Cytoplasmic Ca^{2+} levels in astrocytes are derived from multiple compartments, including endoplasmic reticulum (Kastritsis et al., 1992), mitochondrial sodium-calcium exchange (Parnis et al., 2013), and the extracellular space (Gao et al., 2013). One important mechanism by which $[Ca^{2+}]_i$ can be regulated in astrocytes is by reverse (Ca^{2+}-importing) activity of sodium-calcium exchangers (NCX) (Paluzzi et al., 2007; Reyes et al., 2012), the three isoforms of which are expressed in astrocytes (Minelli et al., 2007).

Recent work has also indicted the importance of $[Na^+]_i$ fluctuations in contributing to astroglial excitability and cellular homeostasis, with a prominent mechanism involving the linkage of transmembrane movements of Na^+ and Ca^{2+} (Parpura and Verkhratsky, 2012; Rose and Krase, 2013, Kirischuk et al., 2012). Glutamate receptors and purinoceptors, as well as voltage-gated sodium channels (VGSCs), are known to play a role in astrocytic Na^+ influx, but the molecular mechanisms controlling cytosolic Na^+ concentrations remain poorly understood (Parpura and Verkhratsky, 2012). Evidence supporting reverse NCX activity as a Ca^{2+} source for astrocytes suggests a potential functional role for astrocytic sodium channels as they relate to $[Ca^{2+}]_i$ fluctuations (Kirischuk et al., 2012). Astrocytes express VGSCs (Sontheimer et al., 1996), and in particular the cardiac isotype $Na_v1.5$ (Black et al., 1998; MacFarlane and Sontheimer, 1998; Black et al., 2010). The functions of VGSCs in astrocytes, which are traditionally considered to be non-excitable, have remained elusive, although Sontheimer et al. (1994) have suggested that these channels provide a pathway for Na^+ to enter the cell to maintain $[Na^+]_i$ at levels necessary for Na^+/K^+-ATPase activity.

We present here evidence supporting a contribution of sodium channel $Na_v1.5$ to astrogliosis in an *in vitro* model of glial mechanical injury. We further implicate fluctuations in $[Ca^{2+}]_i$ due to reverse operation of NCX, triggered by VGSC activity, as the mechanism by which $Na_v1.5$ contributes to the response of astrocytes to mechanical injury. Our results establish a link between the activity of VGSCs and astrogliosis, in particular, by way of alterations in $[Ca^{2+}]_i$.

Materials and Methods

Cell Culture

Cells used in all experiments were purified rat primary cortical astrocytes from E19 Sprague-Dawley rats (Invitrogen, Grand Island, NY), which were thawed and maintained per manufacturer's recommendations. The cells were plated on either glass coverslips in 24-well plates (Corning, Tewksbury, MA) or 35 mm glass bottom dishes (MatTek, Ashland, MA) at a seeding density of $\sim 2\times 10^4$ cells. Cells were grown until confluent in astrocyte medium [Dulbecco's modified Eagle's medium +4.5 g/L D-glucose, +L-glutamine, +110 mg/L sodium pyruvate (Invitrogen) supplemented with 15% fetal bovine serum (Hyclone, Rockford, IL), penicillin (100 U/ml) and streptomycin (100 μg/ml) (Invitrogen)]. Greater than 90% of cells in these cultures were GFAP-positive.

Immunocytochemistry

Astrocytes were fixed for 10 min in PFA solution [4% paraformaldehyde (Sigma, St. Louis, MO) in 0.14 M Sorensen's phosphate buffer, pH 7.4], rinsed 3 times, then incubated in blocking solution [phosphate-buffered saline with 3% fish gelatin, 0.3% Triton X-100, and 3% normal donkey serum (all from Sigma)] for 15 min at room temperature. Astrocytes were then incubated with primary antibodies [mouse anti-glial fibrillary acidic protein (GFAP), 1:1000, Covance, Princeton, NJ; rabbit anti-$Na_v1.5$, 1:100, Alomone, Jerusalem, Israel] for 2-3 h at room temperature, rinsed 3 times with phosphate-buffered saline (PBS) and incubated with secondary antibodies [donkey anti-mouse immunoglobulin G-Alexa Fluor 488, 1:1000, Invitrogen; donkey anti-rabbit immunoglobulin G Cy3, 1:500, Jackson ImmunoResearch, West Grove, PA] for 1-2 h at room temperature. Astrocytes were rinsed with PBS and mounted with Aqua Poly mount (Polysciences, Warrington, PA). Control experiments were performed with the omission of the primary antibodies and only background labeling was observed. For $Na_v1.5$/GFAP stained astrocytes, multiple images were accrued with a Nikon C1si confocal microscope (Nikon USA, Melville, NY) operating with frame lambda (sequential) mode and saturation indicator activated to prevent possible bleed-through between channels.

Scratch wound

Astrocytes were plated on glass coverslips in 24-well plastic plates. When confluent, medium was replaced with astrocyte medium (control), astrocyte medium + 10 μM TTX (Calbiochem, San Diego, CA), or astrocyte medium + 0.5 μM KB-R7943 (Calbiochem). The medium was then removed and saved while the astrocytes were mechanically scratched with a pipette tip similar to previous descriptions (e.g. Yu et al., 1993; MacFarlane and Sontheimer, 1997; Környei et al., 2000), yielding a linear cell-free wound. The saved medium was replaced in each well and the cells were incubated under usual conditions for 24 h.

For experiments in which the scratched astrocytes were incubated with TTX for only the initial 15 min or 2 hour time period, cells were rinsed three times with PBS after treatment with TTX for the appropriate time period and incubated with astrocyte medium for the duration of the 24 h experiment.

To investigate the contribution of $[Ca^{2+}]_i$ in response to mechanical injury, the Ca^{2+} chelator Oregon-Green 488 BAPTA-AM (OGB) (Invitrogen) was employed. Cells were incubated with 10 μM OGB with 0.125% pluronic (Invitrogen) in astrocyte medium for 1 h prior to scratch. Twenty-four hours following the mechanical injury, the cells were fixed and processed for detection of GFAP.

Mechanical injury quantification

To quantify the extent of wound closure in the experimental conditions, montages of the entire coverslip were obtained with a Nikon Ti-E inverted microscope (Tokyo, Japan), using a 10× objective. NIS-Elements AR software (Nikon USA, Melville, NY) was used for analysis of the average wound width (μm) of each scratched coverslip by measuring the total area of the cell-free wound and dividing by the length of the major axis. Average wound width in experimental conditions was normalized to the untreated condition for each experiment, to account for variability between cultures. For each experiment, the growth into the initial injury area at t=24 h was calculated as a percentage of the mean initial width of the wound (t=0).

To assay the consistency of the mechanical scratch, coverslips (n=31) were scratched, fixed at t=0, processed for GFAP immunocytochemistry, and imaged; the mean ± SEM initial scratch width was 414 ± 12 μm, indicating consistent initial injury.

$Na_v1.5$ siRNA knockdown scratch wound

Accell siRNA molecules (pool of 4 different sequences, SMARTpool E-089494-00- 0005) targeting rat $Na_v1.5$, as well as non-targeting (NT) control Accell siRNA #1 (D-001910-01-05) were purchased from Thermoscientific (USA) and used at a final concentration of 1 μM according to the manufacturer's protocol. Briefly, siRNA molecules were re-suspended in siRNA buffer (Thermoscientific, USA) and then added to Accell medium to a final concentration of 1 μM. Growth medium was removed from confluent astrocytes and the delivery (two treatment conditions: NT-siRNA in Accell medium and $Na_v1.5$ siRNA in Accell medium) added to cells for 48 h prior to initiation of mechanical injury as described above. Standard cell lysis techniques were then used and the RNA extracted (Samad et al., 2010). Due to variability between cultures, we normalized the results of the wound healing assay to NT siRNA, where there is minimal $Na_v1.5$ knockdown (Fig. 3a)

Quantitative real-time reverse transcription-PCR

Cultured rat primary cortical astrocytes were processed for RNA extraction using RNasy Microkit (Qiagen, Valencia, CA) according to the manufacturer's protocol. Three hundred ng of total RNA was used to generate 1st strand cDNA using Superscript III (Invitrogen) according to the manufacturer's protocol. Real-time Taman PCR assays for rat: $Na_v1.1$ (assay id: Rn00578439_m1), $Na_v1.2$ (Rn00680558_m1), $Na_v1.3$ (Rn01485332_m1), $Na_v1.4$ (Rn01461132_m1), $Na_v1.5$ (Rn00565502_m1), $Na_v1.6$ (Rn00570506_m1), $Na_v1.7$ (Rn00591020_m1), $Na_v1.8$ (Rn00568393_m1), $Na_v1.9$ (Rn00570487_m1), NCX1 (Rn00570527_m1), NCX2 (Rn00589573_m1), NCX3 (Rn01517855_m1) and rat GAPDH (Rn01775763_g1) were used with Universal Taqman PCR master mix (20×) (all from

Applied Biosystems, Carlsbad, CA). One microliter of the cDNA was used as a template in 20 μl and the reaction was run in duplicates according to the manufacturer's instructions using the Eppendorf realplex (USA). Normalization and expression analysis of gene of interest mRNA were done using the 2–δCt method with GAPDH as the control.

Astrocyte migration assay

Astrocytes were plated in 24-well glass bottom dishes and incubated with astrocyte medium, astrocyte medium + 10 μM TTX, or astrocyte medium + 0.5 μM KB-R7943 prior to performing a scrape injury with a cell scraper. After injury, cells were transferred to an incubation chamber on a Nikon Ti-E inverted microscope (Tokyo, Japan). Phase-contrast images of the entire coverslip were obtained at multiple time points over a 24 h period, using a 10× objective. NIS-Elements AR software (Nikon USA, Melville, NY) was used for analysis of the average process extension of each coverslip (μm) by measuring process extension of individual astrocytes from original site of injury. Migration in experimental conditions was normalized to the untreated condition for each experiment, to account for variability between cultures.

$Na_V1.5$ siRNA knockdown migration assay

ON-TARGET plus siRNA molecules (pool of 4 different sequences, SMARTpool L-089491-02) targeting rat $Na_V1.5$ as well as non-targeting control #1 (D-001810-01-05) were purchased from Thermoscientific (USA) and used at a final concentration of 25 nM according to the manufacturer's protocol. Briefly, siRNA molecules were re-suspended in siRNA buffer (Thermoscientific, USA) and then added to Opti-MEM I Reduced Serum Medium (Invitrogen). Separately, Lipofectamine 2000 (Invitrogen) was added to Opti-MEM I Reduced Serum Medium and allowed to incubate for 5 min at RT. The siRNA mixture was then added to the Lipofectamine 2000 mixture and incubated for 20 min at RT. Astrocyte media was removed and delivery media (NT-siRNA/Lipofectamine 2000/Opti-MEM I medium or $Na_V1.5$ siRNA/Lipofectamine 2000/Opti-MEM I medium) was added to the cells overnight. The cells were washed and the delivery media was replaced with astrocyte media and cells incubated for an additional 24 h prior to initiation of the scrape injury.

Astrocyte proliferation assay

BrdU assays were performed to assess cell proliferation per manufacturer's instructions (Sigma). Briefly, control (no mechanical injury) and mechanically scratched astrocytes were incubated with 10 μM BrdU in astrocyte medium. After 24 h, astrocytes were fixed with PFA solution for 15 min, washed three times with PBS, permeabilized with 0.3% Triton X-100 at RT for 15 min, incubated with 2M HCL at 37° C for 30 min, neutralized with 0.1M borate buffer (pH=8.5) three times, and washed three times with PBS. The cells were then incubated in 500 μl PBS/3% normal donkey serum/2% fish gelatin/0.1% Triton X-100 at 37° C for 30 min, incubated with mouse anti-BrdU (1:200, Serotec) and rabbit anti-GFAP (1:1000, Chemicon, Billerica, MA) at 37° C for 30 min, washed three times with PBS, and incubated with donkey anti-mouse immunoglobulin G Cy3 (1:500, Jackson) and donkey anti-rabbit immunoglobulin G Alexa Fluor 488 (Invitrogen) at 37° C for 30 min. The cells were washed five times with PBS and mounted on slides with Aqua Poly mount.

To test the effect of TTX and KB-R7943 on proliferation, the entire procedure was repeated in the presence of these reagents for 24 h. We attempted to assess proliferation following knockdown of $Na_v1.5$ with siRNA, but the astrocytes were not viable following transfection with siRNA plus exposure to BrdU (24 h), and thus proliferation could not be assessed.

To count BrdU-positive cells, NIS-Elements AR software was employed. A 3-5 mm^2 area was assayed for each coverslip, with the analyzed area for scratched coverslips <500 μm from the edge of the wound. The cell-free wound area was subtracted from the total area assayed and data converted to BrdU-positive cells per mm^2, both along the margin of the wound and in unscratched conditions. Each experimental condition was expressed as % proliferation compared to the value for a paired control (unscratched) at 24 h for each experiment to account for variability between cultures.

Measurement of $[Ca^{2+}]_i$ after injury

Astrocytes were maintained in 35 mm glass bottom dishes. Once confluent, cells were loaded with 5 μM Fura-2 AM (Invitrogen) in standard bath solution (SBS; 140 mM NaCl, 3 mM KCl, 1 mM $MgCl_2$, 1 mM $CaCl_2$, 10 mM HEPES, pH 7.3, 320 mOsm) with 0.05% pluronic (Invitrogen) at room temperature for 90 min. For cells in TTX or KB-R7943 treatment conditions, the pharmacologic agents were included in the Fura-2 AM SBS solution. After incubation, cells were rinsed twice with SBS and 2 ml SBS was placed in the dish for the remainder of the experiment. For cells in TTX or KB-R7943 treatment conditions, the pharmacologic agents were included in the 2 ml SBS placed for the duration of the experiment. Cells from a single field per dish were initially imaged with bright-field optics with a Nikon Ti-E inverted microscope. Subsequently, using a NIKON UV-2E/Cfilter cube with the excitation filter removed, cells were illuminated at 340 and 380 nm using filters installed in a fast wavelength switching light source (Lambda DG-4, Sutter Instruments, Novato, CA). The dichroic mirror used was 400 nm LP with a 460/50 bandpass emission filter. Images were captured with a QuantEM CCD camera (Princeton Instruments, Trenton, NJ), and digitized with NIS- Elements AR software (Nikon). 340/380 ratio images were collected every 2 s during the experiments.

To induce mechanical injury in the cultures, cells were scratched in place with a custom quartz injury device. Astrocytes within 50 μm of the scratch edge (~3-4 cells deep) were analyzed using NIS-Elements AR software. Cells were grouped in 50 μm wide laminae due to the synchronous nature of the $[Ca^{2+}]_i$ wave traveling through the syncytium. For each experiment, 10 cells were randomly picked in each laminae as regions of interest (ROI) utilizing bright-field optics and data for emission following 340 nm and 380 nm excitation were extracted for each ROI. Data were background corrected based on levels in the cell-free area at the end of each experiment, after the wound had been initiated. A 340/380 ratio was manually computed for each cell along every time point during the experiment. To normalize all experiments performed on different days, the control basal level for each set of experiments was adjusted to a ratio of 0 and the treated conditions were adjusted by the same value.

$Na_v1.5$ siRNA knockdown $[Ca^{2+}]_i$ measurement after injury

ON-TARGET plus siRNA molecules (pool of 4 different sequences, SMARTpool L-089491-02) targeting rat $Na_v1.5$ mRNA as well as non-targeting control #1 (D-001810-01-05) were purchased from Thermoscientific (USA) and used at a final concentration of 25 nM according to the manufacturer's protocol and as described earlier. Delivery media (NT-siRNA/Lipofectamine 2000/Opti-MEM I medium or $Na_v1.5$ siRNA/ Lipofectamine 2000/Opti-MEM I medium) was added to the cells overnight. The cells were washed and the delivery media was replaced with astrocyte media and cells incubated for an additional 24 h prior to initiation of Fura-2 AM measurements as described above. After completion of the $[Ca^{2+}]_i$ measurements, standard cell lysis techniques were then used and the RNA extracted (Samad et al., 2010).

Statistics

Data are presented as mean ± SEM from n determinations as indicated. Data were analyzed with an unpaired Student t-test or a one-way ANOVA (for >2 groups) followed by Tukey's honest significance test. Significance was reached if $p < 0.05$. All statistics were performed with Origin 9.0 (Origin Lab Corporation, Northampton, MA), with the exception of AUC data for $[Ca^{2+}]_i$ experiments, which was analyzed with GraphPad Prism (La Jolla, CA).

Results

Astrocytes express $Na_v1.5$ and NCX1

Previous studies have reported the expression of $Na_v1.1$, $Na_v1.2$, $Na_v1.3$ (Black et al., 1994), $Na_v1.6$ (Reese and Caldwell, 1999), and notably $Na_v1.5$ sodium channels (Black et al., 1998) in rodent astrocytes. Consistent with these previous studies, we found that rat primary cortical astrocytes *in vitro* express sodium channel $Na_v1.5$ as evidenced by both immunocytochemical (Fig. 1a) and RT-PCR (Fig. 1b) assays. $Na_v1.5$ mRNA expression in astrocytes was robust and significantly greater than that of other VGSC subtypes. Additionally, since it is known that sodium channel activity can drive reverse Na^+/Ca^{2+} exchange in astrocytes (Paluzzi et al., 2007; Kirischuk et al., 2012), we assessed the expression of NCX1, NCX2, and NCX3 in the cultured cortical astrocytes by RT-PCR and observed strong expression of NCX1 mRNA (Fig. 1b).

TTX and KB-R7943 inhibit astroglial response to injury

In order to evaluate the contribution of $Na_v1.5$ and NCX1 in the response of astrocytes following a scratch injury, we first took a pharmacological approach and studied the effect of VGSC blocker (TTX) and NCX inhibitor 2-[2-[4-(4-Nitrobenzyloxy)phenyl]ethyl]isothiourea mesylate (KB- R7943) on the response of astrocytes to physical injury (Fig. 2a). Since $Na_v1.5$ is resistant to block by nanomolar levels of TTX (Rogart et al., 1989), we used a TTX concentration of 10 μM, which is known to block $Na_v1.5$ (Gu et al., 1997; Catterall et al., 2005). A KB-R7943 concentration of 0.5 μM was used, as the reverse mode of NCX is selectively affected at this low dose [IC_{50} = 1.1-3.4 μmol/L for reverse mode and IC_{50} > 30 μmol/L for forward mode (Iwamoto et al., 1996; Persson et al., 2013a, b)]. Twenty-four hours following mechanical injury by sterile pipette

tip (scratch), astrocytes extended into the injury gap, resulting in 54 ± 3% (n=29) closure of the gap compared to the original wound size (t=0) (Fig. 2b, c). Upon addition of TTX, the degree of closure of the gap was attenuated, with blockade of sodium channels resulting in significantly decreased closure of 28 ± 5% of the initial gap area at t=0 (n=15, p=0.00002). Similarly, addition of KB-R7943 inhibited closure of the wound area; regrowth after 24 h was 36 ± 6% of the original wound area (n=6, p=0.03698) (Fig. 2b, c).

To determine whether the inhibitory action of TTX and KB-R7943 was additive, the effect of combined exposure to TTX + KB-R7943 compared to TTX alone was tested in separate experiments. A significant difference between TTX + KB-R7943 and TTX treatments with respect to wound closure was not detected after 24 h (data not shown), consistent with a common pathway for the effects of TTX and KB-R7943 on the response of astrocytes to mechanical injury.

We next determined whether there was a crucial time-frame for the treatment with TTX to inhibit wound closure. In separate experiments, TTX was applied for 15 min (n=5) or 2 h (n=6) after scratch and compared to TTX applied for the full 24 h time period (n=5). After 24 h, there were significant differences between the degree of wound closure for control (54 ± 5%, n=7) and TTX treatment for 15 min (31 ± 5%, n=5), 2 h (31 ± 5%, n=6), and 24 h (30 ± 7%, n=5)(p=0.03740, p=0.02691, and p=0.02668, respectively), compared to original wound size at t=0, but not among the three TTX treatment groups (Fig. 2d). These findings are consistent with an early role of VGSCs in the response of astroglia in wound closure after injury.

$Na_v1.5$ knockdown inhibits astrocyte response to injury

The marked inhibition by 10 μM TTX of the glial response to mechanical injury and our finding that $Na_v1.5$ is the predominant VGSG expressed in cultured rat cortical astrocytes obtained at E19 strongly suggest that the $Na_v1.5$ isotype contributes to the glial response to injury *in vitro*. To demonstrate the involvement of $Na_v1.5$, we took a loss-of- function knockdown approach using a pool of 4 specific siRNA sequences targeting the $Na_v1.5$ mRNA. $Na_v1.5$ knockdown after siRNA treatment was confirmed by quantitative real-time RT-PCR, and showed that $Na_v1.5$ mRNA expression of cells treated with $Na_v1.5$ siRNA was significantly decreased by 70 ± 11% compared to non-targeting (NT) siRNA (p=0.01252), indicating successful knockdown of $Na_v1.5$ (Fig. 3a). To confirm the specificity of the $Na_v1.5$ siRNA cocktail on $Na_v1.5$ mRNA expression, we performed real-time RT-PCR. Minimal effects of NT siRNA or $Na_v1.5$ siRNA treatment on the expression of Nav1.2, Nav1.6 and Nav1.7 mRNA were observed (Fig. 3b).

Due to variability between cultures, we normalized the results of the wound healing assay to NT siRNA, where there is minimal $Na_v1.5$ knockdown (Fig. 3a). Twenty-four hours after the scratch injury, we found that exposure to $Na_v1.5$ siRNA (n=6) reduced the amount of wound closure to 45 ± 15% compared to NT siRNA (n=6, p=0.01346) (Fig. 3c, d).

Astrocyte response to injury is due to migration and proliferation and both processes are attenuated by TTX and KB-R7943

Previous studies have shown that astrogliosis *in vivo* involves cell proliferation and elongation of cell processes (Faulkner et al., 2004; Wanner et al., 2013). To determine the cellular processes contributing to scratch wound closure in our experiments, we first assessed the presence of migrating cells after injury using live imaging microscopy. After a scrape-induced injury (Fig. 4a, boundary of initial injury indicated by red line), cell process extension was observed throughout the 24 h time period. After 24 h, cell processes had migrated 136 ± 20 μm from the site of injury in control conditions. Compared to controls (n=9), treatment with TTX decreased this migration by 21 ± 3% (n=3, p=0.04708) and treatment with KB- R7943 decreased migration by 30 ± 6% (n=5, p=0.00256) (Fig. 4b). Similarly, astrocytes treated with NT siRNA (n=4) migrated 143 ± 6 μm from the site of injury. Treatment with $Na_v1.5$ siRNA decreased this 24 h migration by 20 ± 7% (n=3, p= 0.04534) (Fig. 4c)

To determine whether cell proliferation contributed to wound closure, we used a BrdU assay. After 24 h, there was a significant 77 ± 9% increase in proliferation amongst cells along the edge of a scratch (n=7) compared to cells in unscratched cultures (n=8, p=0.000006) (Fig. 5a, b). Additionally, while neither TTX nor KB-R7943 affected rates of cell proliferation in cultures without a scratch compared to untreated cultures (data not shown), both agents significantly decreased proliferation of cells along the edges of a wound. Compared to untreated scratched cultures, TTX decreased proliferation by 54 ± 4% (p=0.00596), while KB-R7943 decreased proliferation in mechanically injured cells by 46 ± 9% (p=0.01991) (Fig. 5b). The effects of TTX and KB-R7943 on attenuation of injury-induced proliferation were of similar magnitude (p=0.96016), consistent with involvement of VGSC and NCX activities along a common pathway. These findings suggest that attenuation of wound closure by TTX and KB-R7943 is due to combined effects on both migration and proliferation.

$[Ca^{2+}]_i$ is necessary for astrocyte response to injury

There is an extensive literature regarding a contribution of $[Ca^{2+}]_i$ fluxes for cell migration (Schwab et al., 2012) and proliferation (Berridge, 1995) in numerous cell types, including astrocytes (Stanimirovic et al., 1995; Wang et al., 2010; Parnis et al., 2013). Given the similar effects of TTX and KB-R7943 on the response of astrocytes to mechanical injury and the non-additivity of their effects, we considered a common pathway involving changes in $[Ca^{2+}]_i$ due to reverse operation of NCX triggered by increased $[Na^+]_i$ via VGSCs, specifically $Na_v1.5$. To test this hypothesis, we first determined whether astroglial response to mechanical injury was dependent on $[Ca^{2+}]$ levels. An intracellular Ca^{2+} chelator, Oregon-Green 488 BAPTA-AM (OGB), was loaded into astrocytes before a scratch injury was performed. After 24 h, OGB-treated cells exhibited only minimal growth into the scratched area (mean gap width = 395 ± 65 μm, n=4), compared to the t=0 scratched area (mean gap width = 414 ± 12 μm, n=31), thereby demonstrating a requirement for $[Ca^{2+}]_i$ levels in the response of astrocytes to mechanical injury.

Astrocytes display a robust $[Ca^{2+}]_i$ response after injury, which is attenuated by TTX and KB- R7943

Given the effect of TTX and KB-R7943 on the response of astrocytes to scratch injury, and the requirement for $[Ca^{2+}]_i$ levels in astrogliosis, we examined $[Ca^{2+}]_i$ dynamics with the calcium indicator Fura-2 AM in astrocytes after mechanical injury. After scratch injury, there was a robust $[Ca^{2+}]_i$ response that propagated through the syncytium of confluent astrocytes, and slowly resolved after 2-4 min (Fig. 6a, first panel; Fig. 6b, red line, Video 1). To determine whether blockade of sodium channels and reverse NCX altered the injury-induced $[Ca^{2+}]_i$ transient in astrocytes, we treated the cells with TTX and KB-R7943 prior to injury and assessed the $[Ca^{2+}]_i$ response. TTX and KB-R7943 each attenuated the initial $[Ca^{2+}]_i$ increase after injury, particularly within the first 60 s (Fig. 6a-c; Videos 2, 3). Compared to untreated and scratched control astrocytes (n=7 experiments, 70 cells total), TTX decreased the initial 60 s area under curve (AUC) by 21 ± 5% (n=3 experiments, 30 cells total, p=0.01065), while KB-R7943 decreased the initial 60 s AUC by 20 ± 1% (n=3 experiments, 30 cells total, p=0.01355) (Fig. 6c). In addition, TTX decreased the peak $[Ca^{2+}]_i$ transient by 16 ± 3% (p=0.00395) and KB-R7943 decreased the peak $[Ca^{2+}]_i$ by 12 ± 3% (p=0.02109) compared to scratched and untreated astrocytes (Fig. 6d). There were not significant differences between the inhibitory effects of TTX and KB-R7943 on the initial 60 s AUCs or the peak Ca^{2+} transients (p=0.9913 and p=0.6613, respectively), consistent with a common pathway contributing to attenuation of $[Ca^{2+}]_i$ response after injury.

$Na_v1.5$ knockdown attenuates astrocytic $[Ca^{2+}]_i$ response after injury

In light of the inhibitory effect of TTX on injury-induced $[Ca^{2+}]_i$ response in astrocytes and the attenuation of wound closure following $Na_v1.5$ siRNA incubation, we determined whether knockdown of $Na_v1.5$ would yield similar attenuation of Ca^{2+} transients in mechanically injured astrocytes. Quantitative real-time RT-PCR confirmed that $Na_v1.5$ mRNA expression of cells treated with $Na_v1.5$ siRNA was decreased by 68 ± 5% compared to NT siRNA (p=0.00002), indicating successful knockdown of $Na_v1.5$ (Fig. 7e). Compared to NT siRNA (n=3 experiments, 30 cells total), $Na_v1.5$ siRNA (n=5 experiments, 50 cells total) treatment significantly attenuated the $[Ca^{2+}]_i$ response after injury (Fig. 7a, b; Videos 4, 5). Specifically, knockdown of $Na_v1.5$ decreased the initial 60 s AUC by 18 ± 2% (p=0.00461, Fig. 7c) and the peak $[Ca^{2+}]_i$ by 18 ± 3% (p=0.04395, Fig. 7d) compared to NT siRNA. These inhibitory effects on Ca^{2+} transients following $Na_v1.5$ siRNA treatment are similar to those obtained with TTX treatment (AUC decreased 21 ± 5% and peak $[Ca^{2+}]_i$ decreased 16 ± 3%).

Discussion

The molecular mechanisms that control astroglial scarring following CNS insult are complex and an area of active investigation. Homeostatic functions of astrocytes by way of Na^+ and Ca^{2+} signaling play important roles in both physiological and pathological states (Parpura and Verkhratsky, 2012). Here we show, in an *in vitro* model of mechanical injury to astrocytes, that voltage-gated sodium channel (VGSC) $Na_v1.5$, traditionally viewed as a cardiac sodium channel, contributes to the astrocytic response to the insult via triggering

reverse mode of the Na^+/Ca^{2+} exchanger (NCX). Our study provides support for a contribution of VGSCs in the pathway leading to astrogliosis following mechanical injury.

The present study contributes to a large body of work investigating the mechanisms that regulate the glial response to injury, both *in vitro* and *in vivo* (for review, see Sofroniew, 2009), which has led to the identification of several critical molecules, and thus potential targets for the modulation of astrogliosis. For example, signal transducer and activator of transcription 3 (STAT3) regulates astrogliosis after crush spinal cord injury (SCI) by promoting proliferation and elongation of astrocytes along glial scar borders (Herrmann et al., 2008; Wanner et al., 2013). The transcription factor Olig2 has also been identified as an important player in astrogliosis by regulating astrocyte proliferation after cortical contusion injury (Chen et al., 2008), and the transcription factor NF-κβ was found to markedly affect astrogliosis in both spinal cord injury and experimental autoimmune encephalitis (EAE) (Brambilla et al., 2005; Brambilla et al., 2009). The implications of modulation of astrogliosis have been explored by targeting these and other molecules in transgenic and knockout *in vivo* models, and both beneficial (Herrmann et al., 2008; Wanner et al., 2013) and deleterious (Okada et al., 2006, Brambilla et al., 2005; Brambilla et al., 2009) effects have been identified, indicating the heterogeneity of astrogliosis and the complexity of its effects.

Voltage-gated sodium channels contribute to regulation of motility, invasion, and proliferation in numerous cell types (for a review of the non-canonical functions of VGSCs see Black and Waxman, 2013), including immune cells such as macrophages (Carrithers et al., 2009), microglia (Black and Waxman, 2012), lymphocytes (Fraser et al., 2008), and dendritic cells (Kis-Toth et al., 2011). $Na_v1.6$ sodium channels are expressed in association with intracellular membranes within macrophages and appear to participate in pathways that regulate motility of these cells by causing shifts of intracellular Na^+ and Ca^{2+}, which affect signaling pathways, linking VGSC activation to effects on the cytoskeleton (Carrithers et al., 2009). Consistent with a contribution of VGSC activity to cell motility, blockade of VGSCs with TTX attenuates migration of microglia (Black and Waxman, 2012) and invasiveness of T-lymphocytes, with $Na_v1.5$ specifically being implicated (Fraser et al., 2008). In addition, expression of VGSCs in dendritic cells contributes to a depolarized membrane potential that is necessary for cell migration (Kis-Toth et al., 2011). Additionally, VGSCs and NCX have been implicated in GABA-induced NG2 cell migration by way of fluxes in $[Ca^{2+}]_i$ (Tong et al., 2009), and $Na_v1.5$ was shown to be involved in both migration (Wu et al., 2008) and proliferation (Wu et al., 2006) of gastric epithelial cells. In addition to the importance of VGSCs in cell motility and proliferation, it is becoming increasingly recognized that the expression of VGSCs correlates with invasiveness and metastatic potential in many types of cancer cells including prostate (Fraser et al., 2003), breast (Brackenbury et al., 2007; Gillet et al., 2009), and colon (House et al., 2010). Importantly, SCN5A (encoding $Na_v1.5$) has been identified as a driver of human cancer cell invasion in both breast and colon cancer. Electrophysiological analysis of breast cancer cells uncovered sustained $Na_v1.5$ activity (Gillet et al., 2009), and knockdown of $Na_v1.5$ (Brackenbury et al., 2007; Gillet et al., 2009; House et al., 2010) attenuates invasive behavior of these non-excitable cell types. Voltage-gated sodium channels, and specifically $Na_v1.5$, have also been directly linked to $[Ca^{2+}]_i$

shifts in various non-excitable cell types. $Na_v1.5$ in human macrophages regulates the processing of Mycobacteria via organelle polarization and Ca^{2+} oscillations (Carrithers et al., 2011), and it was recently shown that the gene encoding the pore-forming subunit of $Na_v1.5$ triggers a $[Ca^{2+}]_i$ signal that is essential for the positive selection of $CD4^+$ T cells (Lo et al., 2012).

Our results build upon earlier work which demonstrated upregulated expression of $Na_v1.5$ within scarring astrocytes in multiple sclerosis lesions and in other human brain pathologies (Black et al. 2010) and showed that cultured astrocytes display TTX-resistant sodium currents after mechanical injury-induced gliosis (MacFarlane and Sontheimer, 1998). Voltage-gated sodium channel activation leads to increased Na^+ influx, which has the capability to increase $[Ca^{2+}]_i$ via the reverse mode of NCX. Because the reversal potential of NCX in astrocytes is set at levels close to the resting membrane potential (Kirischuk et al., 1997; Reyes et al., 2012), NCX can rapidly switch into reverse mode in response to small $[Na^+]_i$ increases and/or depolarization (Paluzzi et al., 2007; Kirischuk et al., 2012). Simultaneous Ca^{2+} and Na^+ waves have in fact been observed after mechanical and electrical stimulation of cultured astrocytes (Bernardinelli et al., 2004). Furthermore, it has been shown that mechanical strain injury increases intracellular sodium and leads to reversal of NCX in cortical astrocytes (Floyd et al., 2005).

It is widely accepted that cell migration is a Ca^{2+}-dependent process, as many components of the migration apparatus are Ca^{2+}-sensitive, including calcineurin, calpain, and Ca^{2+}/calmodulin-dependent protein kinase, among others (for review, see Schwab et al., 2012). The initiation of cell motility following injury is dependent on an initial wound- induced increase in $[Ca^{2+}]_i$, which induces the transcriptional activity of immediate early genes such as c-fos and c-jun (Tran et al., 1999). These genes have been shown to be important for regulating cell motility in endothelial cells through secondary genes coding molecules involved in cellular migration (Tran et al., 1999). Intriguingly, a recent study identified a signaling cascade that contributes to glial scarring in an *in vitro* mechanical injury model similar to ours. Gao et al. (2013) showed that the $[Ca^{2+}]_i$ increase in astrocytes after injury activates the protein kinase JNK, which phosphorylates transcription factor c-jun to facilitate the binding of AP-1 to the GFAP gene promoter, which in turn allows GFAP upregulation and subsequent scar formation. It is also evident that Ca^{2+} signaling is crucial to the process of cellular proliferation by activating immediate early genes that activate the cell cycle in resting cells (for review, see Berridge, 1995). Given this literature, we suggest that the attenuation of initial $[Ca^{2+}]_i$ response by TTX and KB-R7943 impacts longer-term scar formation by affecting transcriptional activity of immediate early genes (e.g. via JNK/c-jun/AP-1 signaling cascade), which regulate secondary genes important for cell migration and cell proliferation. In support of this proposed mechanism, we found no significant difference between the effects of TTX treatment for 15 minutes versus 2 hours versus 24 hours, indicating that the time-frame for blockade of VGSCs to affect wound closure is early, which corresponds to the early $[Ca^{2+}]_i$ response. Additionally, treatment with the Ca^{2+} chelator Oregon-Green 488 BAPTA-AM (OGB) at the time of cellular injury inhibited the astrocyte response to scratch injury, again indicting the initial $[Ca^{2+}]_i$ increase as a regulator of astrocyte wound closure.

Since astrocytes are highly coupled via gap junctions, supporting conduction of Na^+, Ca^{2+}, and other molecules (Spray et al., 2006; Parpura and Verkhratsky, 2012) to adjacent astrocytes (Konietzko and Miller, 1994), we propose that mechanical injury depolarizes injured cells along the edge of the scratch, and that this depolarization spreads via gap junctions to neighboring cells, activating $Na_v1.5$ and further increasing $[Na^+]_i$ and/or depolarization. The increased intracellular Na^+ gradient would be expected to drive NCX in reverse, or Ca^{2+} importing, mode, thereby increasing $[Ca^{2+}]_i$, and leading to wound closure by Ca^{2+}-dependent migration and proliferation mechanisms, including activation of gene transcription as detailed in Gao et al. (2013) (Fig. 8).

Reactive astrogliosis is an important aspect of most CNS pathologies and although milder forms of astrogliosis may have beneficial effects to the healing of the CNS, it is possible that attenuating the more severe glial scar formation could be beneficial in disease states such as multiple sclerosis, traumatic brain injury (TBI), and spinal cord injury (SCI). Previous studies on *in vivo* models of multiple sclerosis have shown improved clinical status and reduction of axonal loss following treatment with a variety of VGSC blockers including phenytoin (Black et al., 2007), lamotrigine (Bechtold et al., 2006), carbamazepine (Black et al., 2007), safinamide, and flecainide (Morsali et al., 2013). Interestingly, flecainide, which is a Class Ic cardiac anti-arrhythmic, has strong state-dependent effects on $Na_v1.5$ (Ramos et al., 2004). Additionally, phenytoin protects spinal cord axons, reduces gray and white matter destruction surrounding the lesion, and improves functional recovery after contusion-induced SCI (Hains et al., 2004) and phenytoin, riluzole, and mexilitine were all shown to improve outcome after spinal cord injury in rodents (Ates et al., 2007). Whether an attenuation of astrogliosis due to sodium channel blockade contributes to the improved outcomes is not clear.

In summary, our observations in astrocytes *in vitro* demonstrate a molecular mechanism involving VGSC and NCX that contributes to the glial response to injury. Specifically, our results show that reverse Na^+/Ca^{2+} exchange, triggered by $Na_v1.5$ channels, plays an important role in pathways regulating the response of astrocytes to injury.

Supplementary Material

Refer to Web version on PubMed Central for supplementary material.

Acknowledgments

This work was supported by grants from the Rehabilitation Research Service and Medical Research Service, Department of Veterans Affairs (S.G.W.). The Center for Neuroscience and Regeneration Research is a collaboration of the Paralyzed Veterans of America with Yale University. L.W.P. was supported in part by the Medical Scientist Training Grant (NGM007205) from the National Institute of General Medical Studies, National Institutes of Health. We thank Mark Estacion and Shujun Liu for excellent technical assistance.

References

Agulhon C, Petravicz J, McMullen AB, Sweger EJ, Minton SK, Taves SR, Casper KB, Fiacco TA, McCarthy KD. What is the role of astrocyte calcium in neurophysiology? Neuron. 2008; 59:932–946. [PubMed: 18817732]

Ates O, Cayli SR, Gurses I, Turkoz Y, Tarim O, Cakir CO, Kocak A. Comparative neuroprotective effect of sodium channel blockers after experimental spinal cord injury. J Clin Neurosci. 2007; 14:658–665. [PubMed: 17532502]

Bechtold DA, Miller SJ, Dawson AC, Sun Y, Kapoor R, Berry D, Smith KJ. Axonal protection achieved in a model of multiple sclerosis using lamotrigine. J Neurol. 2006; 252:1542–1551. [PubMed: 17219031]

Bernardinelli Y, Magistretti P, Chatton JY. Astrocytes generate Na^+ -mediated metabolic waves. Proc Natl Acad Sci U S A. 2004; 101:4937–14942.

Berridge MJ. Calcium signalling and cell proliferation. BioEssays. 1995; 17:491–500. [PubMed: 7575490]

Black JA, Waxman SG. Noncanonical roles of voltage-gated sodium channels. Neuron. 2013; 80:280–291. [PubMed: 24139034]

Black JA, Waxman SG. Sodium channels and microglial function. Exp Neurol. 2012; 234:302–315. [PubMed: 21985863]

Black JA, Dib-Hajj S, Cohen S, Hinson AW, Waxman SG. Glial cells have heart: rH1 Na^+ channel mRNA and protein in spinal cord astrocytes. Glia. 1998; 23:200–208. [PubMed: 9633805]

Black JA, Liu S, Carrithers M, Carrithers LM, Waxman SG. Exacerbation of experimental autoimmune encephalomyelitis after withdrawal of phenytoin and carbamazepine. Ann Neurol. 2007; 62:21–33. [PubMed: 17654737]

Black JA, Newcombe J, Waxman SG. Astrocytes within multiple sclerosis lesions upregulate sodium channel $Na_V1.5$. Brain. 2010; 133:835–846. [PubMed: 20147455]

Black JA, Westenbroek R, Ransom BR, Catterall WA, Waxman SG. Type II sodium channels in spinal cord astrocytes in situ: immunocytochemical observations. Glia. 1994; 12:219–227. [PubMed: 7851989]

Brackenbury WJ, Chioni AM, Diss JKJ, Djamgoz MB. The neonatal splice variant of $Na_V1.5$ potentiates *in vitro* invasive behaviour of MDA-MB-231 human breast cancer cells. Breast Cancer Res Treat. 2007; 101:149–160. [PubMed: 16838113]

Brambilla R, Persaud T, Hu X, Karmally S, Shestopalov VI, Dvoriantchikova G, Ivanov D, Nathanson L, Barnum SR, Bethea JR. Transgenic inhibition of astroglial NF-kappa B improves functional outcome in experimental autoimmune encephalomyelitis by suppressing chronic central nervous system inflammation. J Immunol. 2009; 182:2628–40. [PubMed: 19234157]

Brambilla R, Bracchi-Ricard V, Hu WH, Frydel B, Bramwell A, Karmally S, Green EJ, Bethea JR. Inhibition of astroglial nuclear factor kappaB reduces inflammation and improves functional recovery after spinal cord injury. J Exp Med. 2005; 4:145–56. [PubMed: 15998793]

Carrithers LM, Hulsberg P, Sandor M, Carrithers MD. The human macrophage sodium channel $Na_V1.5$ regulates mycobacteria processing through organelle polarization and localized calcium oscillations. FEMS Immunol Med Microbiol. 2011; 63:319–327. [PubMed: 22092558]

Carrithers MD, Chatterjee G, Carrithers LM, Offoha R, Iheagwara U, Rahner C, Graham M, Waxman SG. Regulation of podosome formation in macrophages by a splice variant of the sodium channel SCN8A. J Biol Chem. 2009; 284:8114–8126. [PubMed: 19136557]

Catterall WA, Golden AL, Waxman SG. International Union of Pharmacology. XLVII. Nomenclature and structure-function relationships of voltage-gated sodium channels. Pharmacol Rev. 2005; 57:397–409. [PubMed: 16382098]

Faulkner JR, Herrmann JE, Woo MJ, Tansey KE, Doan NB, Sofroniew MV. Reactive astrocytes protect tissue and preserve function after spinal cord injury. J Neurosci. 2004; 24:2143–2155. [PubMed: 14999065]

Floyd CL, Gorin FA, Lyeth BG. Mechanical strain injury increases intracellular sodium and reverses Na^+/Ca^{2+} exchange in cortical astrocytes. Glia. 2005; 51:35–46. [PubMed: 15779085]

Fraser SP, Salvador V, Manning EA, Mizal J, Altun S, Raza M, Berridge RJ, Djamgoz MBA. Contribution of functional voltage-gated Na^+ channel expression to cell behaviors involved in the metastatic cascade in rat prostate cancer: I. Lateral motility. J Cell Physiol. 2003; 195:479–487. [PubMed: 12704658]

Fraser SP, Diss JKJ, Lloyd LJ, Pani F, Chioni AM, George AJT, Djamgoz MBA. T-lymphocyte invasiveness: control by voltage-gated Na^+ channel activity. FEBS Lett. 2008; 569:191–194. [PubMed: 15225632]

Gao K, Wang CR, Jiang F, Wong AY, Su N, Jiang JH, Chai RC, Vatcher G, Teng J, Chen J, Jiang YW, Yu AC. Traumatic scratch injury in astrocytes triggers calcium influx to activate the JNK/c-Jun/AP-1 pathway and switch on GFAP expression. Glia. 2013; 61:2063–2077. [PubMed: 24123203]

Gillet L, Roger S, Besson P, Lecaille F, Gore J, Bougnoux P, Lalmanach G, Guennec JYL. Voltage-gated sodium channel activity promotes cysteine cathepsin-dependent invasiveness and colony growth of human cancer cells. J Biol Chem. 2009; 284:8680–8691. [PubMed: 19176528]

Gu XQ, Dib-Hajj S, Rizzo MA, Waxman SG. TTX-sensitive and -resistant Na^+ currents, and mRNA for the TTX-resistant rH1 channel, are expressed in B104 neuroblastoma cells. J Neurophysiol. 1997; 77:236–246. [PubMed: 9120565]

Hains BC, Saab CY, Lo AC, Waxman SG. Sodium channel blockade with phenytoin protects spinal cord axons, enhances axonal conduction, and improves functional motor recovery after contusion SCI. Exp Neurol. 2004; 188:365–377. [PubMed: 15246836]

Hermann JE, Imura T, Song B, Qi J, Ao Y, Nguyen TK, Korsak RA, Takeda K, Akira S, Sofroniew MV. STAT3 is a critical regulator of astrogliosis and scar formation after spinal cord injury. J Neurosci. 2008; 28:7231–7243. [PubMed: 18614693]

House CD, Vaske CJ, Schwartz AM, Obias V, Frank B, Luu T, Sarvazyan N, Irby R, Strausberg RL, Hales TG, Stuart JM, Lee NH. Voltage-gated Na^+ channel SCN5A is a key regulator of a gene transcriptional network that controls colon cancer invasion. Cancer Res. 2010; 70:6957–6967. [PubMed: 20651255]

Iwamoto T, Watano T, Shigekawa M. A novel isothiourea derivative selectively inhibits the reverse mode of Na^+/Ca^{2+} exchange in cells expressing NCX1. J Biol Chem. 1996; 271:22391–22397. [PubMed: 8798401]

Kastritsis CHC, Salm AK, McCarthy K. Stimulation of the P2Y purinergic receptor on type 1 astroglia results in inositol phosphate formation and calcium mobilization. J Neurochem. 1992; 58:1277–1284. [PubMed: 1548464]

Kirischuk S, Kettenmann H, Verkhratsky A. Na^+/Ca^{2+} exchanger modulates kainate-triggered Ca^{2+} signaling in Bergmann glial cells in situ. FASEB J. 1997; 11:566–572. [PubMed: 9212080]

Kirischuk S, Parpura V, Verkhratsky A. Sodium dynamics: another key to astroglial excitability? Trends Neurosci. 2012; 35:407–506.

Kis-Toth K, Hajdu P, Bacskai I, Szilagyi O, Pappa F, Szanto A, Posta E, Gogolak P, Panyi G, Rajnavolgyi E. Voltage-gated sodium channel Nav1.7 maintains the membrane potential and regulates the activation and chemokine-induced migration of a monocyte-derived dendritic cell subset. J Immunol. 2011; 187:1273–1280. [PubMed: 21715690]

Konietzko U, Miller CM. Astrocytic dye coupling in rat hippocampus: topography, developmental onset, and modulation by protein kinase C. Hippocampus. 1994; 4:297–306. [PubMed: 7842053]

Környei Z, Czirok A, Vicsek T, Madarasz E. Proliferative and migratory responses of astrocytes to *in vitro* injury. J Neurosci Res. 2000; 61:421–429. [PubMed: 10931528]

Lo WL, Donermeyer DL, Allen PM. A voltage-gated sodium channel is essential for the positive selection of CD4(+) T cells. Nature Immunol. 2012; 13:880–887. [PubMed: 22842345]

MacFarlane SN, Sontheimer SH. Spinal cord astrocytes display a switch from TTX-sensitive to TTX-resistant sodium currents after injury-induced gliosis *in vitro*. J Neurophysiol. 1998; 79:2222–2226. [PubMed: 9535982]

Minelli A, Castaldo P, Gobbi P, Salucci S, Magi S, Amoroso S. Cellular and subcellular localization of Na^+-Ca^{2+} exchanger protein isoforms, NCX1, NCX2, and NCX3 in cerebral cortex and hippocampus of adult rat. Cell Calcium. 2007; 41:221–234. [PubMed: 16914199]

Morsali D, Bechtold D, Lee Woojin, Chahdry S, Palchaudhur U, Hassoon P, Snell DM, Malpass K, Piers T, Pocock J, Roach A, Smith KJ. Safinamide and flecainide protect axons and reduce microglial activation in models of multiple sclerosis. Brain. 2013; 136:1067–1082. [PubMed: 23518709]

Okada S, Nakamura M, Katoh H, Miyao T, Shimazaki T, Ishii K, Yamane J, Yoshimura A, Iwamoto Y, Toyama Y, Okano H. Conditional ablation of Stat3 or Socs3 discloses a dual role for reactive astrocytes after spinal cord injury. Nat Med. 2006; 12:829–34. [PubMed: 16783372]

Paluzzi S, Alloisio S, Zappettini S, Milanese M, Raiteri L, Nobile M, Bonanno G. Adult astroglia is competent for Na^+/Ca^{2+} exchanger-operated exocytotic glutamate release triggered by mild depolarization. J Neurochem. 2007; 103:1196–1207. [PubMed: 17935604]

Parnis J, Montana V, Martinex-Delgado I, Matyash V, Parpura V, Kettenmann H, Sekler I, Nolte C. Mitochondrial exchanger NCLX plays a major role in the intracellular Ca^{2+} signaling, gliotransmission, and proliferation of astrocytes. J Neurosci. 2013; 33:7206–7219. [PubMed: 23616530]

Parpura V, Verkhratsky A. Homeostatic function of astrocytes: Ca^{2+} and Na^+ signalling. Transl Neurosci. 2012; 3:334–344. [PubMed: 23243501]

Persson AK, Liu S, Faber CG, Merkies IS, Black JA, Waxman SG. Neuropathy-associated Nav1.7 variant I228M impairs integrity of dorsal root ganglion neuron axons. Ann Neurol. 2013a; 73:140–5. [PubMed: 23280954]

Persson AK, Kim I, Zhao P, Estacion M, Black JA, Waxman SG. Sodium channels contribute to degeneration of dorsal root ganglion neurites induced by mitochondrial dysfunction in an in vitro model of axonal injury. J Neurosci. 2013b; 33:19250–61. [PubMed: 24305821]

Ramos E, O'Leary ME. State-dependent trapping of flecainide in the cardiac sodium channel. J Physiol. 2004; 560:37–49. [PubMed: 15272045]

Reese KA, Caldwell JH. Immunocytochemical localization of NaCh6 in cultured spinal cord astrocytes. Glia. 1999; 26:92–96. [PubMed: 10088676]

Reyes RC, Verkhratsky A, Parpura V. Plasmalemmal Na^+/Ca^{2+} exchanger modulates Ca^{2+}-dependent exocytotic release of glutamate from rat cortical astrocytes. ASN Neuro. 2012; 4:e00075. [PubMed: 22268447]

Rogart RB, Cribbs LL, Muglia LK, Kephart DD, Kaiser MW. Molecular cloning of a putative tetrodotoxin-resistant rat heart Na^+ channel isoform. Proc Natl Acad Sci U S A. 1989; 86:8170–8174. [PubMed: 2554302]

Rolls A, Shecter R, Schwartz M. The bright side of the glial scar in CNS repair. Nat Rev Neurosci. 2009; 10:235–241. [PubMed: 19229242]

Rose CR, Krase C. Two sides of the same coin: sodium homeostasis and signaling in astrocytes under physiological and pathophysiological conditions. Glia. 2013; 61:1191–1205. [PubMed: 23553639]

Samad OA, Tan AM, Cheng X, Foster E, Dib-Hajj SD, Waxman SG. Virus-mediated shRNA knockdown of Na(v)1.3 in rat dorsal root ganglion attenuates nerve injury- induced neuropathic pain. Mol Ther. 2013; 21:49–56. [PubMed: 22910296]

Schwab A, Fabian A, Hanley PJ, Stock C. Role of ion channels and transporters in cell migration. Physiol Rev. 2012; 92:1865–1913. [PubMed: 23073633]

Silver J, Miller JH. Regeneration beyond the glial scar. Nat Rev Neurosci. 2004; 5:146–156. [PubMed: 14735117]

Sofroniew M. Molecular dissection of reactive astrogliosis and glial scar formation. Trends Neurosci. 2009; 32:638–647. [PubMed: 19782411]

Sontheimer H, Black JA, Waxman SG. Voltage-gated Na^+ channels in glia: properties and possible functions. Trends Neurosci. 1996; 19:325–331. [PubMed: 8843601]

Spray DC, Ye ZC, Ransom BR. Functional connexin “hemichannels”: a critical appraisal. Glia. 2006; 54:758–773. [PubMed: 17006904]

Stanimirovic DB, Ball R, Mealing G, Morley P, Durkin JP. The role of intracellular calcium and protein kinase C in endothelin-stimulated proliferation of rat type I astrocytes. Glia. 1995; 15:119–130. [PubMed: 8567063]

Tong XP, Li XY, Zhou B, Shen W, Zhang ZJ, Xu TL, Duan S. Ca^{2+} signaling evoked by activation of Na^+ channels and Na^+/Ca^{2+} exchangers is required for GABA-induced NG2 cell migration. J Cell Biol. 2009; 186:113–128. [PubMed: 19596850]

Tran POT, Hinman LE, Unger GM, Sammak PJ. A wound-induced $[Ca^{2+}]_i$ increase and its transcriptional activation of immediate early genes is important in the regulation of cell motility. Exp Cell Res. 1999; 246:319–326. [PubMed: 9925747]

Wang HH, Hsieh HL, Yang CM. Calmodulin kinase II-dependent transactivation of PDGF receptors mediates astrocytic MMP-9 expression and cell motility induced by lipoteichoic acid. J Neuroinflammation. 2010; 7:84–100. [PubMed: 21092323]

Wanner IB, Anderson MA, Song B, Levin J, Fernandez A, Gray-Thompson Z, Ao Y, Sofroniew MV. Glial scar borders are formed by newly proliferated, elongated astrocytes that interact to corral inflammatory and fibrotic cells via STAT3- dependent mechanisms after spinal cord injury. J Neurosci. 2013; 33:12870–12886. [PubMed: 23904622]

Wu KKL, Li GR, Wong HPS, Hui MKC, Tai EKK, Lam EKY, Shin VY, Ye YN, Li P, Yang YH, Luo JC, Cho CH. Involvement of Kv1.1 and $Na_V1.5$ in proliferation of gastric epithelial cells. J Cell Physiol. 2006; 207:437–444. [PubMed: 16331678]

Wu KKL, Li GR, Wong TM, Wang JY, Yu L, Cho CH. Involvement of voltage-gated K+ and Na^+ channels in gastric epithelial cell migration. Mol Cell Biochem. 2008; 308:219–226. [PubMed: 17978865]

Yu AC, Lee YL, Eng LF. Astrogliosis in culture: I. The model and the effect of antisense oligonucleotides on glial fibrillary acidic protein synthesis. J Neurosci Res. 1993; 34:295–303. [PubMed: 8455207]

Zamanian JL, Xu L, Foo LC, Nouri N, Zhou L, Giffard RG, Barres BA. Genomic analysis of reactive astrogliosis. J Neurosci. 2012; 32:6391–6410. [PubMed: 22553043]

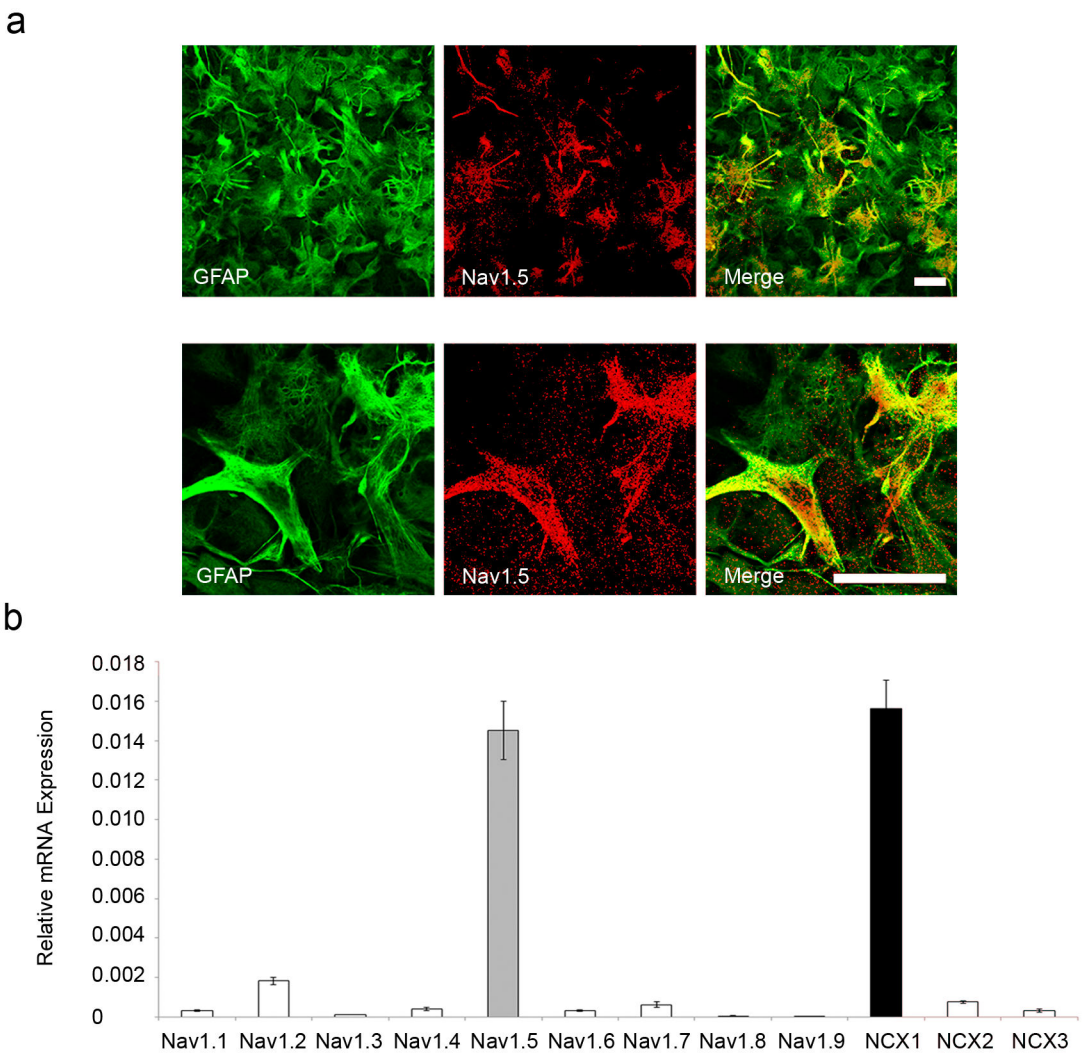

Figure 1.

$Na_v1.5$ and NCX1 expression in astrocytes. **(a)** GFAP positive cultured rat cortical astrocytes (green) exhibit prominent $Na_v1.5$ immunolabelling (red), observed at low magnification (top panel) and at increased magnification (bottom panel). Merged images of GFAP and $Na_v1.5$ are yellow. Scale bars, 25 μm. **(b)** RT-PCR showing relative mRNA expression of VGSC and NCX. $Na_v1.5$ is the predominant VGSC subtype expressed in cultured rat cortical astrocytes and the NCX1 isoform is also robustly expressed.

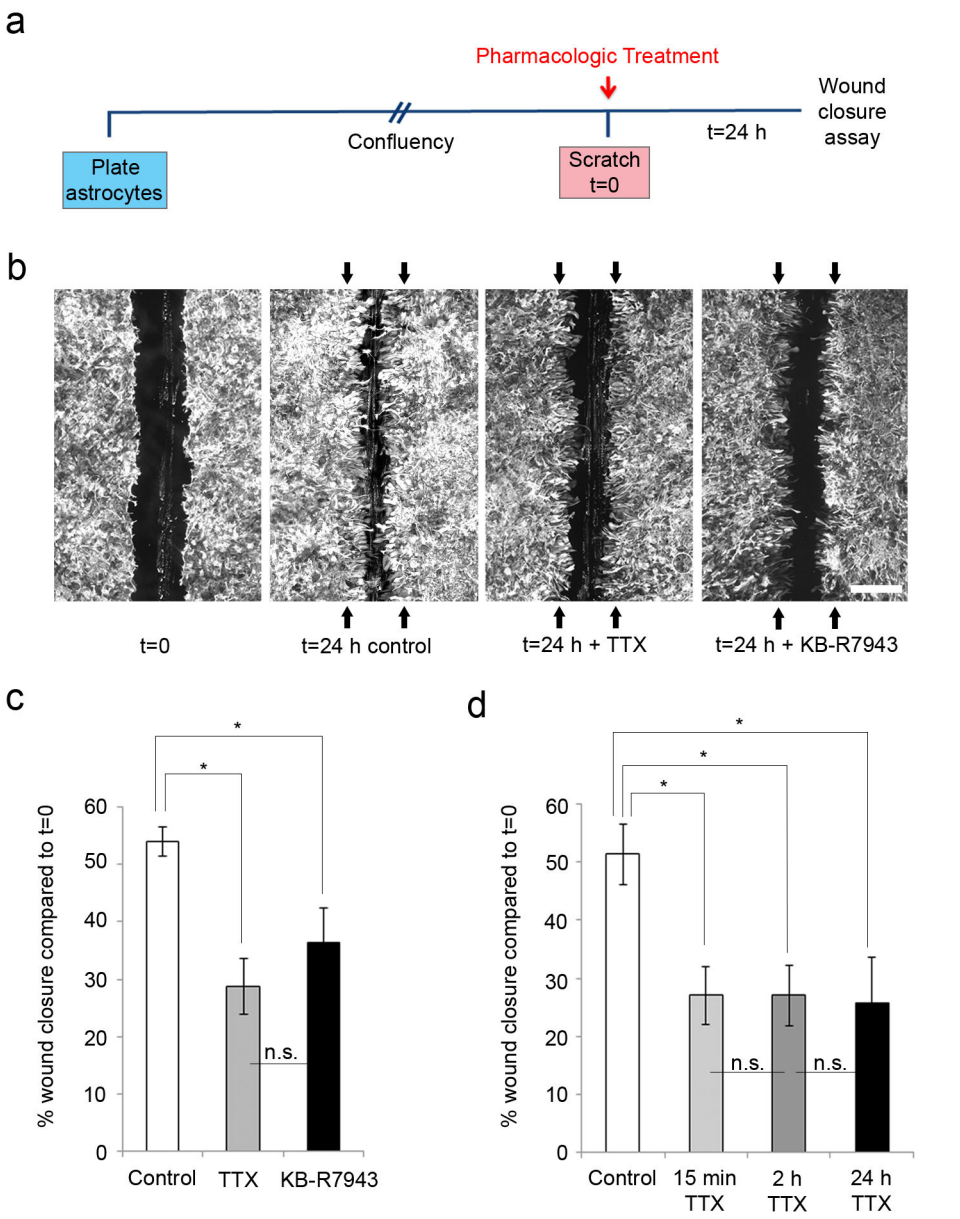

Figure 2.

Astrocyte response to mechanical injury is inhibited by TTX and KB-R7943. **(a)** Schematic of experimental design. Astrocytes were plated and allowed to grow until confluent, at which point they were treated with either TTX or KB-R7943 and scratched. After 24 h, wound closure was analyzed and compared to initial wound size. **(b, c)** Astrocytes grew together following scratch injury, resulting in 54 ± 3% (n=29) closure of the wound compared to the average original wound size (represented by black arrows) after a 24 h time period. TTX treatment attenuated closure of the scratch wound to 28 ± 5% (n=15) of the initial wound size at t=24 h. Similarly, KB-R7943 inhibited wound closure, with 36 ± 6% regrowth (n=6) of the initial scratch size. **(d)** TTX, applied for 15 min or 2 h after scratch, was compared to TTX applied for the full 24 h time period prior to assessment at 24 h. After 24 h, there were significant differences between the degree of wound closure for untreated

scratched controls (54 ± 5%, n=7) and for TTX treatment for 15 min (31 ± 5%, n=5), 2 h (31 ± 5%, n=6), and 24 h (30 ± 8%, n=5). There was no significant difference between the effects of TTX for 15 min, 2 h, and 24 h. Scale bar, 400 μm. *p<0.05; n.s., not significant.

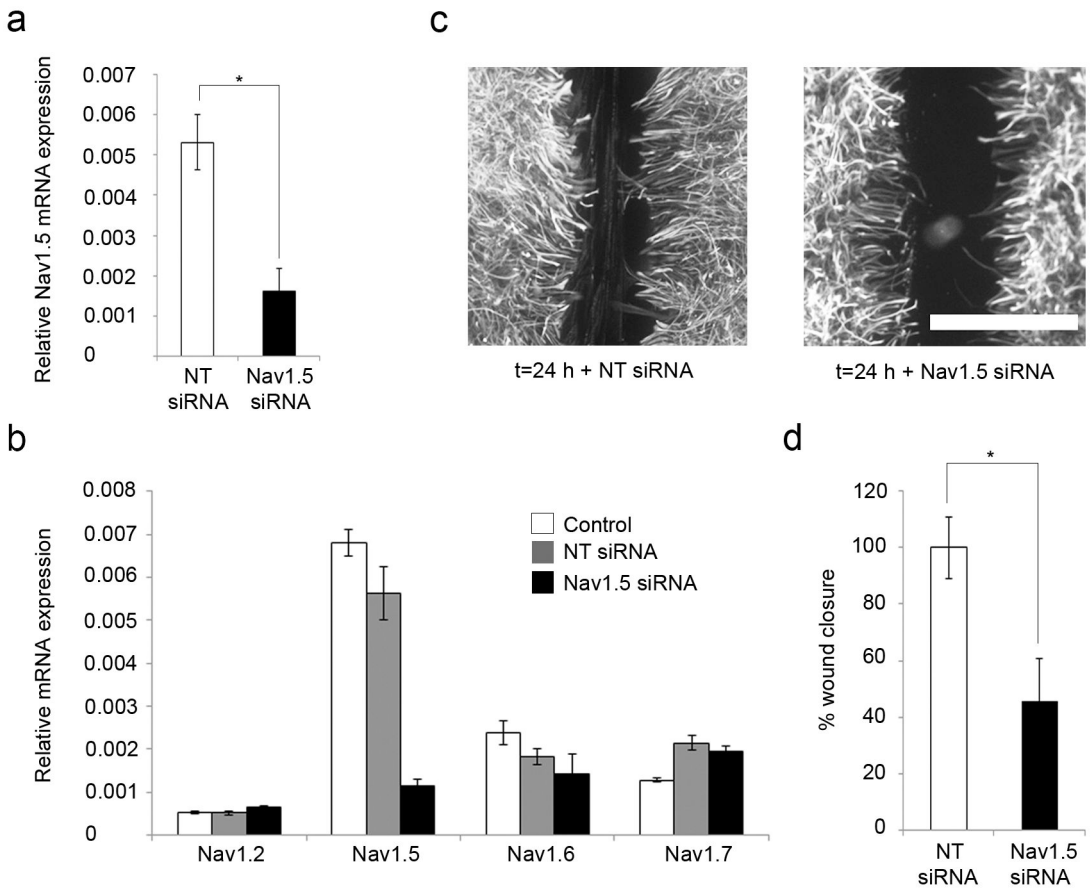

Figure 3.

Astrocyte response to injury is inhibited by $Na_v1.5$ mRNA knockdown. **(a)** To confirm $Na_v1.5$ knockdown after siRNA treatment, quantitative real-time RT-PCR was performed, and showed that $Na_v1.5$ mRNA expression of cells treated with $Na_v1.5$ siRNA was decreased by 70 ± 11% compared to NT siRNA, indicating successful knockdown of $Na_v1.5$. **(b)** Specificity of the $Na_v1.5$ siRNA cocktail on $Na_v1.5$ mRNA expression was confirmed with real-time RT-PCR analysis. Compared to control (white columns), minimal effects of NT siRNA (gray columns) or $Na_v1.5$ siRNA (black columns) on the expression of Nav1.2, Nav1.6, and Nav1.7 mRNA were observed. **(c, d)** Twenty-four hours after the scratch injury, exposure to $Na_v1.5$ siRNA (n=6) reduced the amount of wound closure to 45 ± 15% compared to NT siRNA (n=6). Scale bar, 400 μm. *$p<0.05$; n.s., not significant.

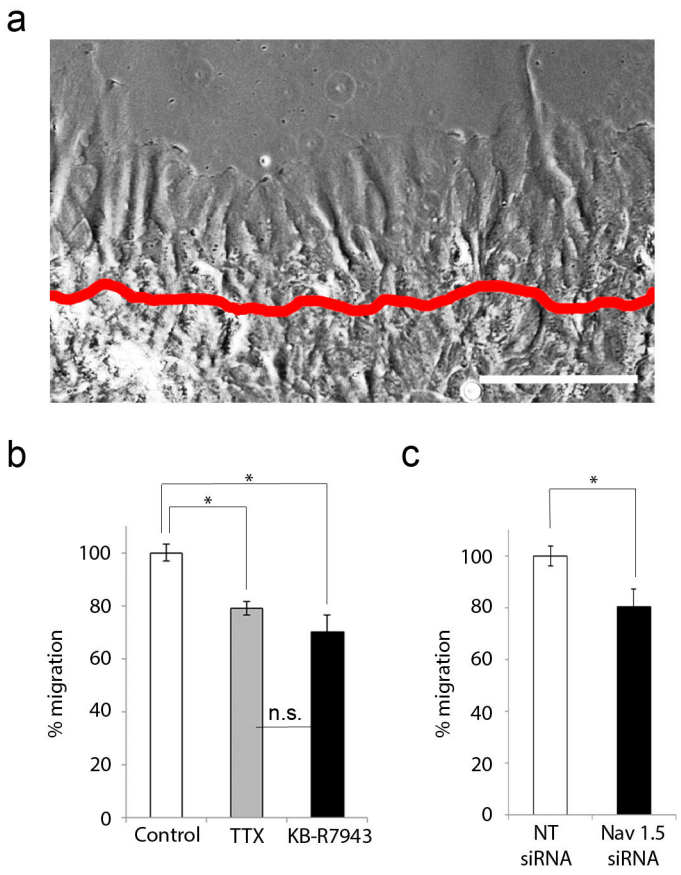

Figure 4.

Astrocyte response to injury involves migration which is attenuated by TTX, KB-R7943, and $Na_V1.5$ mRNA knockdown. **(a)** After a scrape-induced injury (original site of injury marked by red line), astrocytic processes are seen extending. After 24 h, cell processes had migrated 136 ± 20 μm from the site of injury in control conditions. Scale bar, 150 μm. **(b)** Compared to untreated cells (n=9), TTX decreased migration by 21 ± 3% (n=3) and KB-R7943 decreased migration by 30 ± 6% (n=5). **(c)** Compared to treated with NT siRNA (n=4), astrocytes treated with $Na_V1.5$ siRNA exhibited a 20 ± 7% decrease in migration (n=3). *$p<0.05$; n.s., not significant.

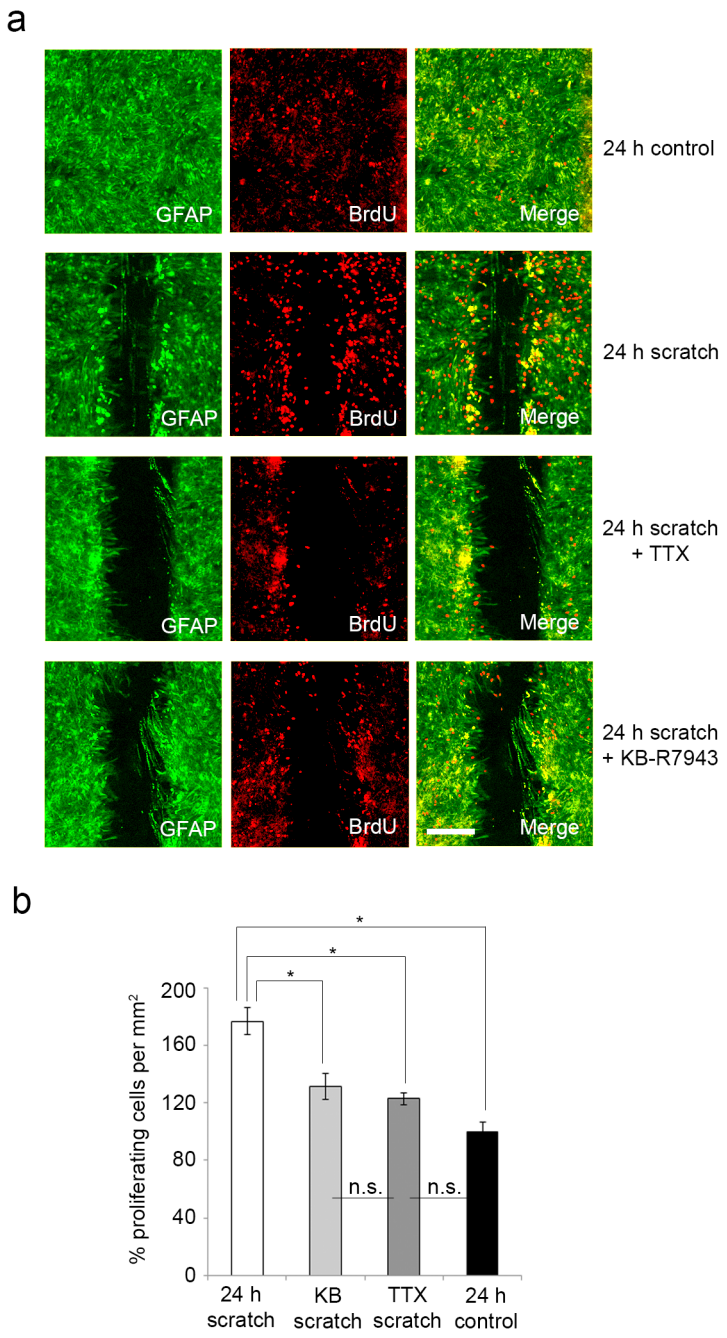

Figure 5.

Astrocyte response to injury involves proliferation which is attenuated by TTX and KB-R7943. **(a)** GFAP positive cultured rat cortical astrocytes (green) exhibit BrdU immunolabelling (red), seen in resting cells (top row) and scratched cells (second row). There is an increase in BrdU-positive cells along the edge of a scratch, which is attenuated with TTX and KB-R7943 treatment (third and fourth rows, respectively). Scale bar 200 μm. **(b)** After 24 h, there was a significant 77 ± 9% increase in proliferation amongst cells along the edge of a wound (n=7) compared to cells in unscratched cultures (n=8), as measured by

BrdU staining. Compared to untreated cells, TTX decreased proliferation by 54 ± 4%, while KB-R7943 decreased proliferation by 46 ± 9%. *$p<0.05$; n.s., not significant.

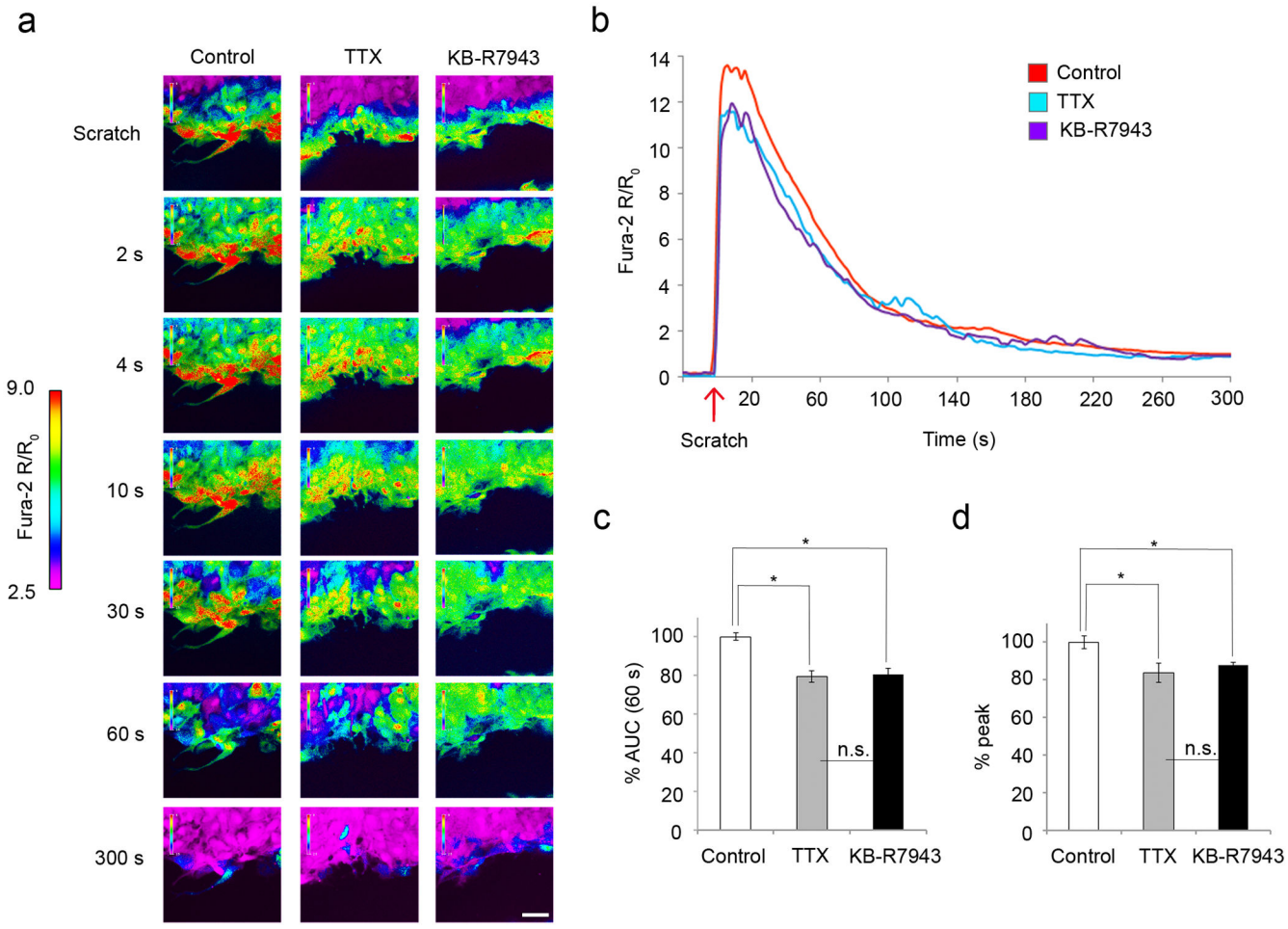

Figure 6.

Astrocytes display robust $[Ca^{2+}]_i$ response after mechanical injury that is attenuated by TTX and KB-R7943. **(a)** After a scratch injury, there was a robust $[Ca^{2+}]_i$ response, which was propagated through the syncytium of confluent astrocytes and slowly resolved after 2-4 min (first column; see also **(b)** and Video 1). Application of TTX and KB- R7943 attenuated this $[Ca^{2+}]_i$ response (second and third columns, respectively, see also **(b)** and Videos 2, 3). Color scale represents the ratio of fluorescent signals induced by 340 and 380 nm excitation in cells loaded with Fura-2 AM. Scale bar, 50 μm. **(b)** TTX and KB-R7943 both attenuated the initial $[Ca^{2+}]_i$ increase after injury, particularly within the first 60 s. **(c)** Compared to untreated scratched astrocytes (n=7 experiments, 70 cells total), TTX decreased the 60 s AUC by 21 ± 5% (n=3 experiments, 30 cells total), while KB-R7943 decreased the 60 s AUC by 20 ± 1% (n=3 experiments, 30 cells total). **(d)** TTX decreased the peak $[Ca^{2+}]_i$ by 16 ± 3%, while KB-R7943 decreased the peak $[Ca^{2+}]_i$ by 12 ± 3%. All data was taken from cells within the first 50 μm (3-4 cells deep) from the scratch. *p<0.05; n.s., not significant.

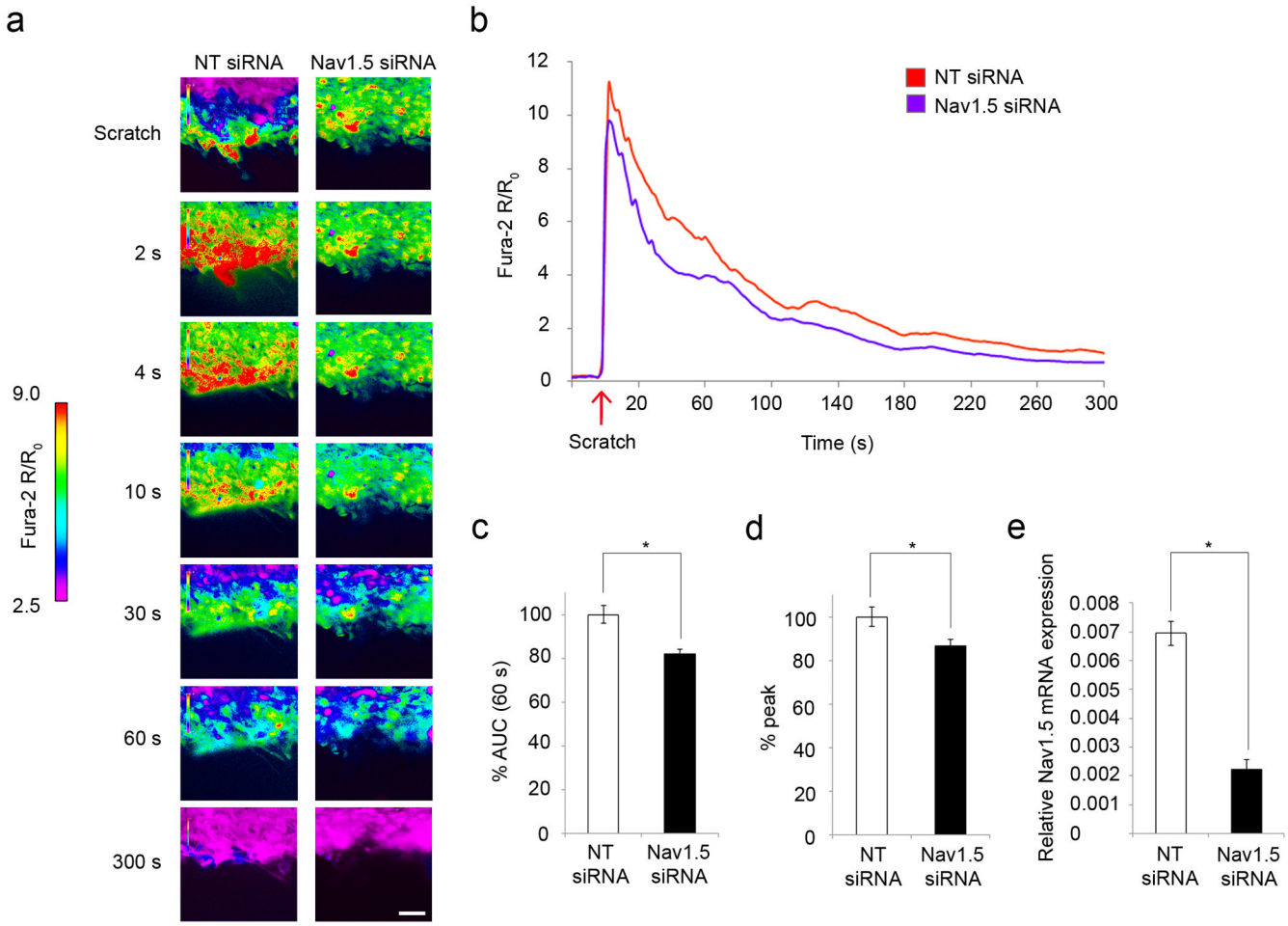

Figure 7.

$Na_v1.5$ mRNA knockdown attenuates astrocytic $[Ca^{2+}]_i$ response after injury. **(a)** After scratch, there was a robust $[Ca^{2+}]_i$ response in cells treated with NT siRNA, which was propagated through the syncytium of astrocytes and slowly resolved after 2-4 min (first column; see also **(b)** and Video 4). Knockdown with $Na_v1.5$ siRNA attenuated the $[Ca^{2+}]_i$ response (second column, see also Video 5) compared to NT siRNA. Color scale represents the ratio of fluorescent signals induced by 340 and 380 nm excitation in cells loaded with Fura-2 AM. Scale bar 50 μm. **(b)** $Na_v1.5$ siRNA attenuated the initial $[Ca^{2+}]_i$ increase after injury, particularly within the first 60 s. **(c)** Compared to NT siRNA control (n=5 experiments, 50 cells total), $Na_v1.5$ siRNA treatment (n=3 experiments, 30 cells total) decreased the 60 s AUC by 18 ± 2%, and **(d)** decreased the peak $[Ca^{2+}]_i$ by 18 ± 3%. **(e)** Quantitative real-time RT-PCR confirmed that $Na_v1.5$ mRNA expression of cells treated with $Na_v1.5$ siRNA was decreased by 68 ± 5% compared to NT siRNA, indicating successful knockdown of $Na_v1.5$. All data was taken from cells within the first 50 μm (3-4 cells deep) from the scratch. *p<0.05.

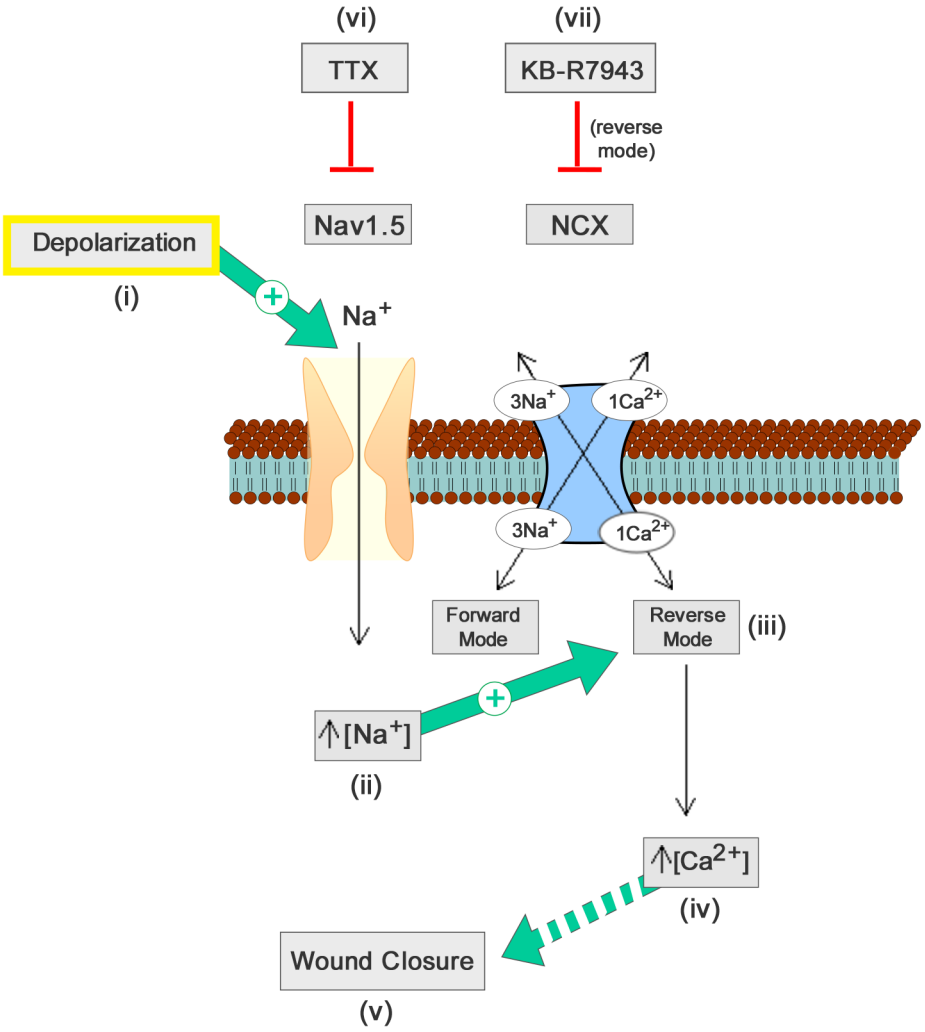

Figure 8.

Schematic of contribution of Nav1.5 and NCX to astrocyte response following scratch injury. Injury-induced depolarization (**i**) activates $Na_v1.5$, which causes an increased $[Na^+]_i$ and further depolarization (**ii**). Increased $[Na^+]_i$ activates the reverse operation of NCX (Ca^{2+}-importing mode) (**iii**), which causes increased $[Ca^{2+}]_i$ (**iv**) that likely acts through multiple pathways (including migration and proliferation) to affect astroglial wound closure (**v**). TTX (**vi**) and KB-R7943 (**vii**) inhibit $Na_v1.5$ and NCX, respectively, thereby attenuating closure of the wound.